Proc. Natl. Acad. Sci. USA
Vol. 91, pp. 4584–4588, May 1994
Biophysics

High-resolution tracking of microtubule motility driven by a single kinesin motor

FADY MALIK*†, DAVID BRILLINGER‡, AND RONALD D. VALE†

*Neuroscience Graduate Program, University of California, San Francisco, CA 94143; †Department of Pharmacology, University of California, San Francisco, CA 94143; and ‡Department of Statistics, University of California, Berkeley, CA 94720

Communicated by Thomas S. Reese, January 26, 1994

ABSTRACT **Kinesin is a microtubule-based motor protein that contains two identical force-generating subunits. The kinesin binding sites along the microtubule lie 8 nm apart (the dimension of the tubulin dimer), which implies that kinesin must translocate a minimum distance of 8 nm per hydrolysis cycle. Measurements of kinesin's microtubule-stimulated ATPase activity (≈20 ATP per sec) and velocity of transport (≈0.6 μm/sec), however, suggest that the net distance moved per ATP (≈30 nm) may be greater than one tubulin dimer under zero load conditions. To explore how kinesin translocates during its ATPase cycle, we constructed a microscope capable of tracking movement with 1-nm resolution at a bandwidth of 200 Hz and used this device to examine microtubule movement driven by a single kinesin motor. Regular stepwise movements were not observed in displacement traces of moving microtubules, although Brownian forces acting on elastic elements within the kinesin motor precluded detection of steps that were <12 nm. Though individual steps of ≈16 nm were occasionally observed, their infrequent occurrence suggests that kinesin rarely moves abruptly by distances of two or more tubulin subunits during its ATP hydrolysis cycle. Instead it is more likely that kinesin moves forward by the distance of only a single tubulin subunit under zero load conditions.**

Kinesin is an ATP hydrolyzing enzyme that translocates membranous organelles along microtubule polymers (1, 2). The mechanism by which cytoskeletal motors such as kinesin and myosin produce movement is unresolved. The most widely accepted theory states that the motor produces unidirectional movement by undergoing a large conformational change (the power stroke) that alters its angle of attachment relative to the polymer (3). This model predicts that motors should produce stepwise movement, with the abrupt displacements corresponding to a power stroke that occurs once per ATPase cycle (4). The distance covered by the power stroke, referred to here as the "step size," is important, because its magnitude places constraints on models for motor mechanism. Step sizes less than the dimensions of the motor domain could be produced by a conventional power stroke model, whereas larger step sizes would suggest that the motor rapidly undergoes multiple mechanical actions per round of ATP hydrolysis (5, 6).

Measurements of the velocity produced by a single kinesin molecule (7, 8) and microtubule-stimulated ATPase rates of kinesin in solution (9–11) suggest that kinesin's step size may be >3-fold larger than the dimension of its force-generating head (9 nm) (12). Such step size calculations are precarious, however, since ATPase rates have not been measured under the same conditions as the motility assay. For these reasons, it is important to measure kinesin translocation along a microtubule by more direct means. Previously, movements of kinesin-coated latex beads along microtubules were analyzed with nanometer accuracy using video microscopy (13); the results showed abrupt 4-nm displacements occurring during translocation at low ATP concentrations. Interpretation of these experiments, however, is complicated by the fact that several kinesin motors were interacting with the microtubule at the same time. In this study, we have tracked microtubule translocation driven by a single kinesin molecule under near-zero load conditions. Our data reveal that kinesin under zero load does not generate >12-nm steps, indicating that movement occurs either by a smooth translocation process or by a series of small stepwise displacements.

The publication costs of this article were defrayed in part by page charge payment. This article must therefore be hereby marked "*advertisement*" in accordance with 18 U.S.C. §1734 solely to indicate this fact.

MATERIALS AND METHODS

Microscope Construction. The microscope is made from optical mounting components (Newport, Fountain Valley, CA) and custom-fabricated parts and is anchored to a vibration isolation table (Newport). A vertically mounted, vibration damped breadboard supports components of the light path. Fig. 1*B* shows a schematic of the microscope; in the following description, numbers in parentheses refer to this schematic. Illumination from a 100-W mercury arc lamp (1) and a 100-mW argon ion laser (2) (model 5490A from Ion Laser Technology, Salt Lake City, UT) operated at 25–50 mW are combined by a dichroic filter (3) (520 LP from Omega Optical, Brattleboro, VT). The arc lamp provides field illumination for imaging purposes. The laser, which is focused onto a spot in the specimen plane (4) coincident with the image plane of the position detector (5), illuminates a 100-nm latex microsphere attached to the microtubule in order to provide sufficient brightness for high-resolution measurements. Radiation pressure on the 100-nm beads was negligible, because free beads in solution were not displaced or trapped by the beam. A 530-nm long-pass filter on a movable slide (6) is positioned in front of the arc lamp during uncaging experiments. Dark-field optics consisted of a 1.2–1.33 numerical aperture (n.a.) reflecting ball condenser (7) and a 40×, 1.0 n.a. DPlanApoUV objective (8), both from Olympus (New Hyde Park, NY). The image from the arc lamp illumination passes through a second dichroic mirror (9) (520 LP) and is directed either to a binocular head or to a silicon intensified target camera (10) (Hamamatsu, Middlesex, NJ), which sends the image to a television monitor and a sVHS video tape recorder. The second dichroic mirror (9) also reflects the laser signal and directs it to a quadrant photodiode (5) (Hamamatsu, S-1557) that functions as a two-dimensional position detector. Four low-noise, high-bandwidth picoamp to voltage converters (AI-403, Axon Instruments, Foster City, CA) transduce the photocurrents, which are then processed by a Cyberamp 380 computer-controlled eight-channel instrumentation amplifier (Axon Instruments). The signals are appropriately added and subtracted in analog form to generate signals proportional to x and y displacement. All data are filtered at 200 Hz with a four-pole Bessel filter, and an analog/digital converter (AT-DIO16-F5; National Instruments, Austin, TX) digitizes the

signals and stores the data on a PC computer. Custom-written software developed using LabWindows (National Instruments) allowed the data to be displayed and further analyzed. The specimen holder was manipulated using a modified, motorized three-axis steel stage (11) (Newport). An *x–y* piezoelectric translator (12) (Physik Instruments, Waldbraun, Germany) driven by a custom-built, low-noise amplifier allows for small translations of the specimen. The detector was calibrated by moving the specimen with the piezoelectric translator and measuring the displacement required at the detector to exactly counterbalance the stage translation. Dividing this displacement by the microscope magnification (330×) at the detector gives the magnitude of the piezoelectric movement.

Protein and Bead Preparation. Kinesin was prepared from squid optic lobe by microtubule affinity and sucrose gradient centrifugation (14). Tubulin was purified from bovine brain and biotinylated according to Hyman *et al.* (15). Carboxylated latex microspheres (Interfacial Dynamics, Portland, OR) were labeled by activating the bead surface with 1-ethyl-3-(3-(dimethylamino)propyl)carbodiimide and sulfo-*N*-hydroxysuccinimide, washing away the free crosslinker by successive centrifugations, adding free strepavidin (1 mg/ml), and then repeated washing of the beads by centrifugation to remove the uncrosslinked protein. To prepare bead-labeled microtubules, tubulin and biotin tubulin (4:1 ratio) were combined to a final total tubulin concentration of 6 mg/ml in microtubule buffer (80 mM KPipes, pH 6.8/1 mM $MgCl_2$/1 mM EGTA) supplemented with 3 mM $MgCl_2$, 10% dimethyl sulfoxide, and 1 mM GTP, and polymerized at 37°C; after 20 min, taxol was added to 16 μM. To remove unpolymerized tubulin, the microtubules were centrifuged (20 min at 12,000 rpm in a microfuge) through a cushion of 40% sucrose in microtubule buffer with 16 μM taxol. Strepavidin-labeled beads at various dilutions were added immediately to the resuspended microtubules (≈3 mg/ml), and the number of beads attached per microtubule was examined several hours later.

Motility Assays. The multiple motor assay was performed by adsorbing kinesin to a density of ≈4 molecules per μm^2 on a casein-coated glass surface of a microscope perfusion chamber (7, 16). Bead-labeled microtubules were then perfused into the chamber in a low ionic strength motility buffer (10 mM Tris·HCl, pH 7.0/3 mM $MgCl_2$/1 mM EGTA/0.1 mM EDTA), which was found to reduce the noise of the microtubule measurements, perhaps by increasing the affinity of kinesin for the glass surface. After 2–5 min, the unattached microtubules and beads in the solution were removed by perfusing the chamber with the above motility buffer containing 16 μM taxol, 0.1% methylcellulose, and either 200 μM ATP or 50 μM ATP. Measurements were made by positioning the moving microtubules (3–8 μm in length) in the center of the photodiode detector with the motorized stage. For the single motor experiments, kinesin was adsorbed at a density of 0.25 molecule per μm^2. To make measurements at this single motor density, 200 μM 3-*O*-[1-(2-nitrophenyl)ethyl]-ester ATP (NPE caged ATP; Molecular Probes) was used instead of ATP, and a UV cutoff filter was placed in the light path of the mercury arc lamp. The microtubule-bound bead was centered on the photodiode detector, and the UV filter was briefly removed from the path to uncage ATP in the observation field. Microtubule movement was also simultaneously videotaped during high-resolution measurements for later evaluation.

Data Analysis. An analysis algorithm was developed to look for periodic features in the data. Since microtubules often moved diagonally across the photodiode, the microtubule's displacement (512 msec of data) was calculated by projecting the *x* and *y* components along a unit vector parallel to the direction of microtubule travel. A line was robustly fitted to the displacement trace (17), and residual values were calculated. A Fourier transform was performed on these data, and the modulus was determined. In preparation for averaging data from several microtubules, a robustly fitted line was subtracted from logarithmic spectral values at low frequencies, which resulted in flat spectra. Since microtubules were traveling at somewhat different velocities, the spectra were normalized by transforming frequency into displacement (velocity/frequency) before being averaged together. The significance (*P* value) of the resulting maximum peak was calculated using a periodogram analysis. The resolving power of this algorithm was tested by applying it to a set of 16 traces in which either a smooth line or periodic 8-nm steps (filtered at 200 Hz) simulating a 200 μm/sec velocity were added to different traces of rigor kinesin–microtubule complexes. The analysis was also tested by varying the time interval between steps using a Gamma probability distribution (a generalized form of the Poisson distribution).

RESULTS

Measurements of Kinesin–Microtubule Complexes in the Absence of ATP. To track kinesin-driven movement with high spatial and temporal resolution, we built an inverted dark-field microscope, which was optimized for stability, vibration immunity, and maximal light transmission. A quadrant photodiode array was used to track two-dimensional movements since it provided better temporal resolution than a video camera (Fig. 1*B* and *Materials and Methods*). The resolution of the microscope (determined by using stationary beads firmly fixed onto the slide surface) was ≈1 nm at a 200-Hz bandwidth (Fig. 1*C*); this noise in the position measurement was probably due to mechanical vibration of the microscope. By attaching a 100-nm bead to a microtubule via a strepavidin-biotin linkage, the displacement of moving microtubules transported by surface-bound kinesin molecules could also be measured with high resolution. As the magnified image of the microtubule-bound bead moved across the photodetector, the individual photocurrents were converted into voltage signals proportional to *x* and *y* position. The displacement measurement was linear over ≈0.4 μm (data not shown), a distance of ≈50 tubulin dimers.

Before examining translocating microtubules, we first analyzed the noise of bead–microtubule complexes held to the glass by surface-adsorbed kinesins in the absence of ATP (Fig. 1*C*). Microtubules held to the glass by kinesin motors in the absence of ATP exhibited greater noise than beads firmly fixed to the glass surface (Fig. 1*C*). This increase reflects flexibility in the attachment between the bead and microtubule and the microtubule with the surface-bound kinesin(s). The kinesin molecule probably represents the most compliant component in the system because strepavidin is small and the microtubule has a stiffness comparable to Plexiglas (18). This notion is supported by the finding that noise increases with decreasing numbers of motors attached to the microtubule. The noise from a single motor attachment is still quite low considering the 80-nm length of kinesin (12), suggesting that the majority of the molecule is well attached to the surface and not just bound at one end. Assuming that the noise is due to thermal agitation of a linear spring within the kinesin molecule, an upper limit on the stiffness of the spring constant (k) of an elastic element within the motor can be estimated. Equating thermal energy ($1/2k_BT$) to potential energy ($1/2k\langle x\rangle^2$, where $\langle x\rangle^2$ is the mean-square displacement along the axis parallel to the rigor kinesin–microtubule complex), gives a value for the kinesin spring constant (0.9×10^{-4} N/m) similar to that obtained for muscle myosin (2.5×10^{-4} N/m) (19).

By measuring microtubules lying parallel to either the *x* or *y* axis of the position detector, we also found that the bead noise perpendicular to the microtubule axis is larger than the parallel component ($P < 0.05$) (Fig. 1*C*). One possible

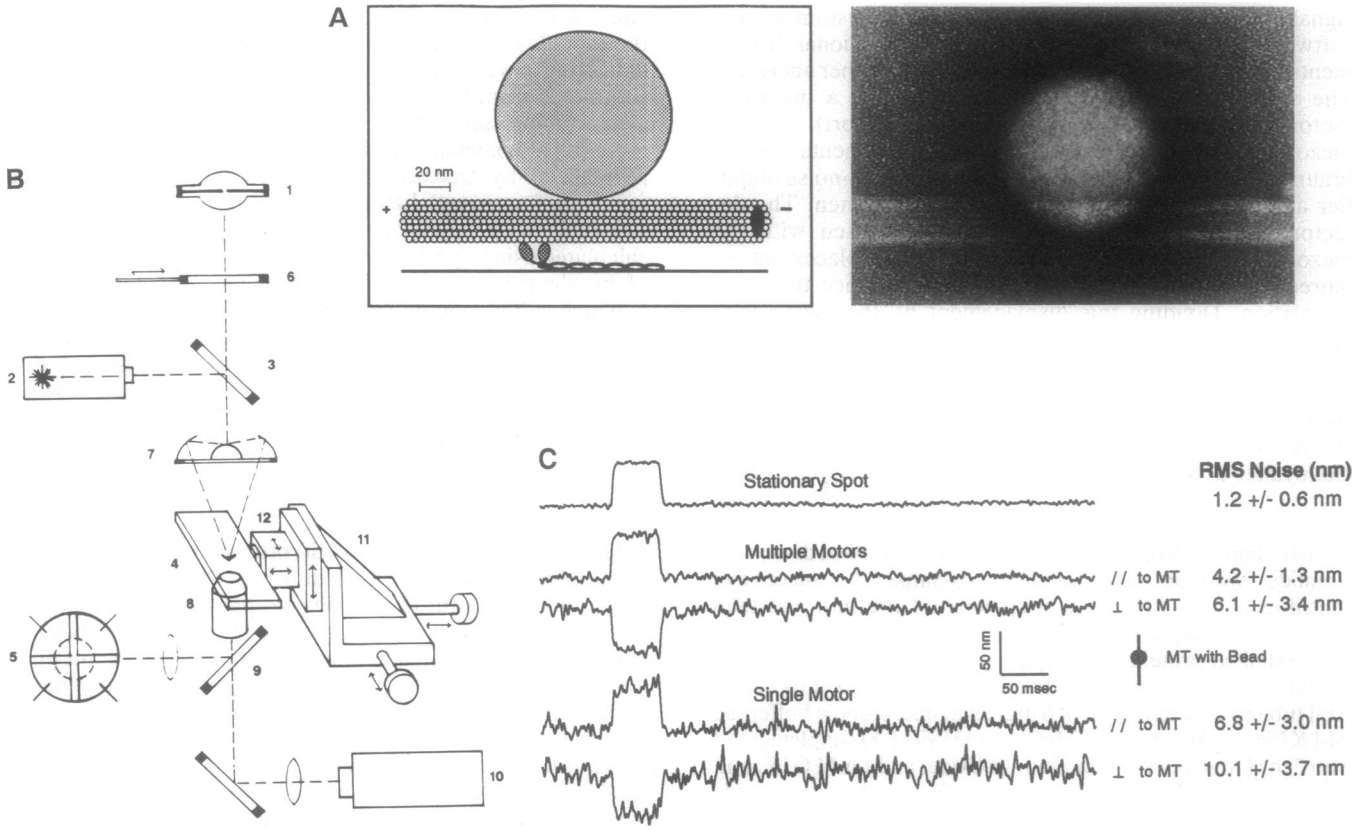

FIG. 1. Motility assay and microscope for high-resolution tracking measurements. (*A*) Schematic of the motility assay in which surface-adsorbed kinesin powers the transport of a microtubule. A single 100-nm strepavidin-coated latex microsphere bound to a biotinylated microtubule (see electron micrograph to the right; ×260,000) serves as a bright marker to determine accurately the microtubule's position. (*B*) Schematic of the custom-built dark-field microscope used for nanometer and millisecond resolution measurements of the bead's position (see text for details). (*C*) Representative displacement traces of a bead firmly attached to the glass (top) and a bead attached to a stationary microtubule held either by several (middle) or a single (bottom) kinesin motor. The average noise values from 15 traces are shown on the right. The square calibration pulse is generated by a piezoelectric translator moving the stage by 50 nm.

explanation for this observation is that the two kinesin motor domains are bound to two different tubulin subunits along one protofilament, which would preferentially diminish the axial Brownian motion of the microtubule.

Measurements of Microtubule Translocation Driven by Multiple or Single Kinesin Motors. To obtain displacement traces, gliding microtubules with attached beads were positioned in the field coincident with the photodiode position detector. Typical high-resolution measurements of microtubule translocation at kinesin densities of 4/μm^2 (estimated to be ≈3–5 kinesins per microtubule) in the presence of 200 μM ATP (microtubule velocity equal to 360 ± 90 nm/sec) or 50 μM ATP (170 ± 60 nm/sec) are shown in Fig. 2 *A* and *B*. The microtubules move in a smooth and continuous manner for the overwhelming majority of the time. The rms noise of these moving bead–microtubule complexes was not substantially different from those analyzed in the absence of ATP. By inspecting the traces in Fig. 2 *A* and *B*, occasional abrupt displacements can be seen, but there was no obvious pattern of stepwise movement.

Since the steplike behavior of individual motors might be damped by having several motors attached to the same microtubule (20), we sought to measure microtubule movement produced by a single kinesin (7, 8). Microtubules were judged to be propelled by a single motor if they displayed pivoting behavior at some time before they detached from the glass and if they traveled for a distance less than their length (7). By these criteria, we found that >90% of the <6-μm-long microtubules were moved by single motors (1- to 2-μm-long microtubules, 96%; 3–4 μm, 91%; 5–6 μm, 87%; 7–8 μm, 73%; 9–10 μm, 70%; n = 340) at the low kinesin density (0.25 μm^2) used for our single motor measurements.

At the kinesin density used to measure single motor motility, microtubules would only move for a few seconds before they detached from the glass; this amount of time was insufficient to align the microtubule on the photodiode. To circumvent this difficulty, the assay was modified so that microtubules were first bound to kinesin in the absence of ATP, then caged ATP was added, and the image of the microtubule-attached bead was aligned on the photodiode. Motility was initiated by releasing ATP with UV illumination. Data were collected from microtubules during short periods (0–1 sec) of linear translocation between times of exhibiting nodal pivoting. It is unlikely that these short periods represent attachment to a second kinesin, since microtubules hardly ever moved beyond their length at this density. Microtubule velocity would vary according to the efficiency of uncaging and the decrease of ATP concentration due to diffusion from the site of activation. Data from high-velocity (275 ± 60 nm/sec, which corresponds to those elicited by ≈200 μM ATP) and lower-velocity (175 ± 40 nm/sec, which corresponds to those elicited by ≈50–70 μM ATP) movements were pooled for later analysis.

As with multiple motors, visual inspection of 100 single motor translocation records revealed no obvious and consistent steplike behavior (Fig. 2 *C* and *D*). To assess what size of step could be visually detected above the background Brownian noise, a series of steps were added to records of stationary microtubules attached to the glass surface by single kinesin motors in the absence of ATP (Fig. 3). Visual inspection by naive observers could reliably detect steps

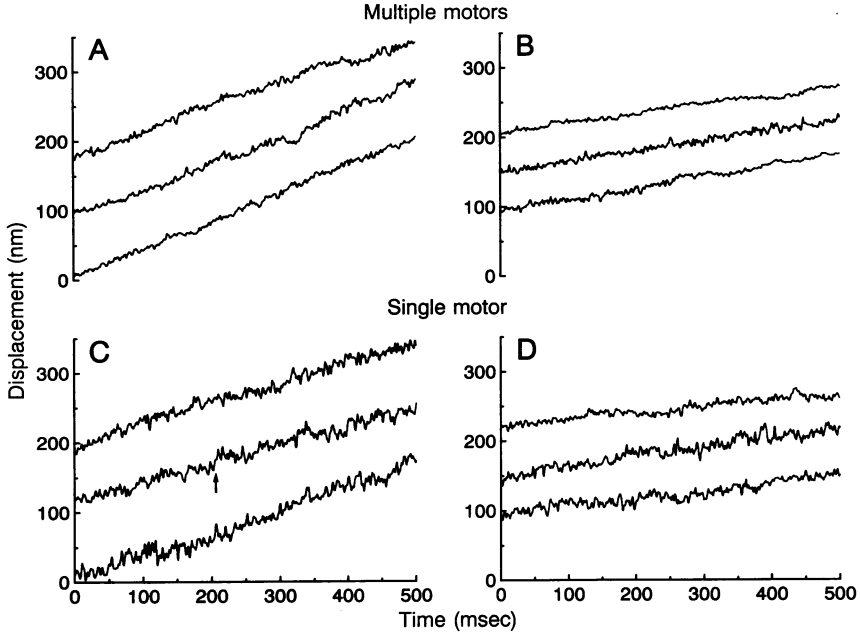

FIG. 2. Representative displacement measurements of kinesin-driven microtubule movement. The upper (*A* and *B*) and lower (*C* and *D*) panels show traces of microtubule movement (component parallel to the microtubule axis) by multiple (three to five motors) and single motors, respectively. Higher-velocity traces are shown in *A* and *C* (≈200 μM ATP) and lower-velocity movements are shown in *B* and *D* (≈50 μM ATP). Although occasional abrupt displacements are observed (arrow), the majority of the traces appeared to display smooth translocation. The rms noise of the traces was 5.3 ± 1.4 nm (*A*), 3.8 ± 0.7 nm (*B*), 9.4 ± 2.1 nm (*C*), and 6.7 ± 1.6 nm (*D*).

added to the data if they were 12 or 16 nm. However, steps of 8 nm in size could not be distinguished above the Brownian noise of the kinesin–microtubule complex.

Since abrupt stepwise movements of ≈12 nm should be evident, we examined our displacement traces for such occurrences. In 48 traces (corresponding to 24 sec of single motor-induced translocation), only 18 step-like displacements between 12 and 25 nm were observed (16 ± 3 nm); stepwise displacements >25 nm were not detected in these sets of data. Since such events were rare, it is difficult to be certain that they are indeed motor-driven translocations, although inspection of modeled rigor data (as in Fig. 3) only revealed 3 steps of >12 nm in 15 sec of data (14 ± 2 nm). This analysis indicates that kinesin rarely moves by distances of two or more tubulin subunits in an abrupt manner.

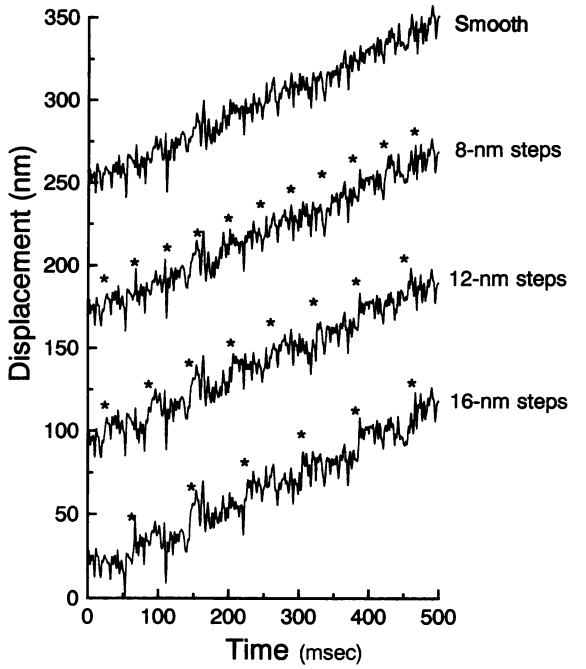

FIG. 3. Model traces containing step translocations. Uniform staircase functions with steps of magnitude indicated to the right were added to traces of stationary microtubules held to the glass surface by single kinesin molecules (see text for details). An example of one trace is shown here. In the top trace, a smooth line was added for comparison. Step translocations are not visually apparent until the step magnitude reaches 12 nm. Asterisks indicate where steps occur.

Fourier Spectral Analysis. To detect steps smaller than visual inspection would allow, a Fourier spectral analysis was employed to look for repetitive features in the traces (Fig. 4). This analysis could easily detect a regular pattern of 8-nm steps added to single motor rigor traces (Fig. 4*B*). A significant peak at the expected frequency also was obtained only when the time interval between 8-nm steps varied with a coefficient of variation of 0.2 or less (Fig. 4*C*). Steps occurring with greater variation in their intervening time interval could not be detected. When this analysis was applied to the single motor moving traces (Fig. 4*D*), no significant peaks were observed, indicating that if the motor takes 8-nm steps then the time interval between these steps probably varies in a stochastic manner.

DISCUSSION

In this study, we have examined with high temporal and spatial resolution the movements of microtubules driven by single kinesin molecules under near-zero load conditions. Our data show that kinesin does not take regular steps >12 nm in length. Occasional stepwise displacements corresponding to the dimensions of two tubulin dimers were observed but were very rare. Thus, it is unlikely that kinesin translocates over multiple tubulin dimers per round of ATP hydrolysis. These results are at variance with the large kinesin step sizes (>30 nm) calculated from transport velocities and microtubule-stimulated ATPase rates (9–11). We favor the explanation that kinesin takes a small step (<12 nm) per ATPase cycle and that the large step size calculations

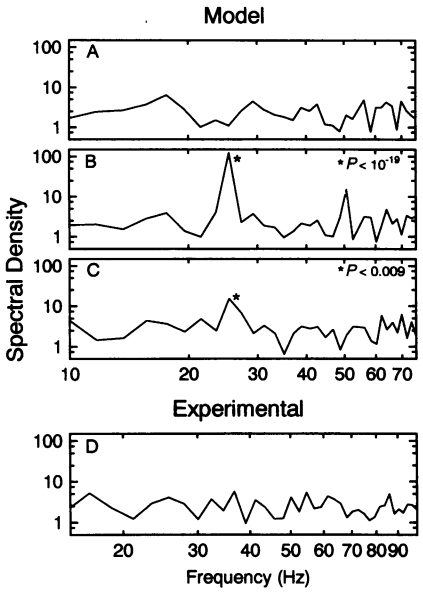

FIG. 4. Fourier spectral analysis to uncover periodic stepping behavior. The significance (*P* value) of the largest peak (indicated by the *) is shown in the upper right of each box (note the logarithmic scales of the plots). (*A*) Average spectrum of modeled data in which a smooth line was added to 16 different stationary kinesin–microtubule complexes. There are no significant peaks. (*B*) Analysis of modeled regular 8-nm steps. There is a large peak at the expected frequency (25 Hz) and its first harmonic (50 Hz). (*C*) Analysis in which the time interval between 8-nm steps varied by as much as 20% (see text). Again, there is a significant peak at the expected frequency. (*D*) Average spectrum of translocating microtubules driven by single motors (14 microtubules, average velocity 275 ± 60 nm/sec). None of the peaks is significant ($P > 0.1$).

reflect difficulties in determining kinesin's maximal ATPase rate. One possibility, for example, is that ATP turnover in the motility assay is higher than the values obtained from solution measurements.

Since kinesin moves along a single microtubule protofilament (13, 21, 22) and only binds to one site per tubulin dimer (23, 24), the minimum distance covered during a kinesin translocation cycle should be 8 nm (the distance between tubulin dimers along a protofilament). Detecting 8-nm steps in our system is difficult, however, since the Brownian motion of the kinesin–microtubule linkage is of comparable magnitude to the size of this step. Diffusion-derived noise could be overcome by averaging a microtubule's position over relatively longer time periods at low velocities [such as in the case of a microtubule moving slowly at low ATP concentrations or in the presence of certain nucleotide analogues (25)]. However, measurements of several seconds were precluded in our single motor assay by the nodal pivoting of the microtubule. In an independent investigation of kinesin motility, Svoboda *et al.* (26) were able to decrease the Brownian noise associated with the kinesin–microtubule complex by generating a load upon the kinesin motor using an optical trap and documented the presence of 8-nm steps under such conditions. Under the near-zero load conditions in our study, it is also likely that the kinesin motor is only moving the distance of a single tubulin dimer per step. Given the dimensions of the relatively small kinesin force-generating domain (≈9 nm) (12), it still remains a challenge to explain how the kinesin motor is able to move a distance comparable to its own size.

We are grateful to Dr. Stephen Smith for his assistance in the early stages of this project. We also thank P. Wong of Newport Instruments and L. Bocskai, O. Teixeira, and D. McVay of the University of California, San Francisco (UCSF) machine shops. L. Romberg and R. Cooke provided helpful comments on the manuscript. J. Schmid provided the illustration of the microscope. This work was supported by grants from the Whitaker Foundation and the National Institutes of Health (GM38499) to R.D.V., the Medical Scientist Training Program to F.M., the National Science Foundation (DMS-9208683) to D.B., and the Lucille P. Markey Charitable Trust to the Program in Biological Sciences to UCSF.

1. Vallee, R. B. & Shpetner, H. S. (1990) *Annu. Rev. Biochem.* **59**, 909–932.
2. Skoufias, D. A. & Scholey, J. (1993) *Curr. Opin. Cell Biol.* **5**, 95–107.
3. Huxley, H. E. (1969) *Science* **164**, 1356–1364.
4. Spudich, J. A. (1990) *Nature (London)* **348**, 284–285.
5. Yanagida, T., Arata, T. & Oosawa, F. (1985) *Nature (London)* **316**, 366–369.
6. Ishijma, A., Doi, T., Sakurada, K. & Yanagida, T. (1991) *Nature (London)* **352**, 301–306.
7. Howard, J., Hudspeth, A. J. & Vale, R. D. (1989) *Nature (London)* **342**, 154–158.
8. Block, S. M., Goldstein, L. S. & Schnapp, B. J. (1990) *Nature (London)* **348**, 348–352.
9. Kuznetsov, S. A. & Gelfand, V. I. (1986) *Proc. Natl. Acad. Sci. USA* **83**, 8350–8354.
10. Hackney, D. D. (1988) *Proc. Natl. Acad. Sci. USA* **85**, 6314–6318.
11. Sadhu, A. & Taylor, E. W. (1992) *J. Biol. Chem.* **267**, 11352–11359.
12. Hirokawa, N., Pfister, K. K., Yorifuji, H., Wagner, M. C., Brady, S. T. & Bloom, G. S. (1989) *Cell* **56**, 867–878.
13. Gelles, J., Schnapp, B. J. & Sheetz, M. P. (1988) *Nature (London)* **331**, 450–453.
14. Schnapp, B. J. & Reese, T. S. (1989) *Proc. Natl. Acad. Sci. USA* **86**, 1548–1552.
15. Hyman, A., Dreschel, D., Kellogg, D., Salser, S., Sawin, K., Steffen, P., Wordeman, L. & Mitchison, T. (1991) *Methods Enzymol.* **196**, 478–485.
16. Romberg, L. & Vale, R. D. (1993) *Nature (London)* **391**, 168–170.
17. Becker, R. A., Chambers, J. M. & Wilks, A. R. (1989) *The New S Language* (Wadsworth, Pacific Grove, CA).
18. Gittes, F., Mickey, B., Nettleton, J. & Howard, J. (1993) *J. Cell Biol.* **120**, 923–934.
19. Huxley, A. F. & Simmons, R. M. (1971) *Nature (London)* **233**, 533–538.
20. Pate, E. & Cooke, R. (1991) *J. Musc. Res. Cell Motil.* **12**, 376–393.
21. Ray, S., Meyhofer, E., Milligan, R. A. & Howard, J. (1993) *J. Cell Biol.* **121**, 1083–1094.
22. Kamimura, S. & Mandelkow, E. (1992) *J. Cell Biol.* **118**, 865–875.
23. Harrison, B. C., Marchese-Ragona, S. P., Gilbert, S. P., Cheng, N., Steven, A. C. & Johnson, K. A. (1993) *Nature (London)* **362**, 73–75.
24. Song, Y.-H. & Mandelkow, E. (1993) *Proc. Natl. Acad. Sci. USA* **90**, 1671–1675.
25. Shimizu, T., Furusawa, K., Ohashi, S., Toyoshima, Y., Okuno, M., Malik, F. & Vale, R. D. (1991) *J. Cell Biol.* **112**, 1189–1197.
26. Svoboda, K., Schmidt, C. F., Schnapp, B. J. & Block, S. M. (1993) *Nature (London)* **365**, 721–727.